Iterative Receiver with Gaussian and Mean-Field Approximation in Massive MIMO Systems

Sheng Wu[1], Linling Kuang[1(✉)], Xincong Lin[1], and Baosheng Sun[2]

[1] Tsinghua Space Center, Tsinghua University, Beijing 100084, China
{thuraya,kll}@tsinghua.edu.cn
[2] Beijing Space Information Relay and Transmission Technology Research Center, Beijing 100094, China

Abstract. In this paper, a computationally efficient message-passing receiver that performs joint channel estimation and decoding is proposed for massive multiple-input multiple-output (MIMO) systems with OFDM modulation. We combine the loopy belief propagation (LBP) with the mean-field approximation and Gaussian approximation to decouple frequency-domain channel taps and data symbols from noisy observations. Specifically, pair-wise joint belief of frequency-domain channel tap and symbol is obtained by soft interference cancellation, after which the marginal belief of frequency-domain channel tap and symbol are estimated from the pair-wise joint belief by the mean-field approximation. To estimate time-domain channel taps between each pair of antennas, a Gaussian message passing based estimator is applied. The whole scheme of joint channel estimation and decoding is assessed by Monte Carlo simulations, and the numerical results corroborate the superior performance of the proposed scheme and its superiority to the state of art.

Keywords: Belief propagation · Channel estimation · Decoding
Massive MIMO · Message passing · Mean-field approximation
Orthogonal frequency-division multiplexing (OFDM)

1 Introduction

Recently, massive MIMO systems with a large number of antennas at the base-station have gained great attention [1–6]. Accurate channel state information (CSI) is essential in massive MIMO systems, as high data rate and energy efficiency are achievable only when CSI is known. In TDD mode, the available training resources are limited by the channel coherence interval [7]. In contrast to conventional MIMO systems with a small number of antennas, the overhead required for channel estimation in massive MIMO systems may be overwhelming. Therefore, accurate channel estimation with reduced overhead is critical to massive MIMO systems.

This work was supported by the National Nature Science Foundation of China (Grant No. 91438206 and Grant No. 91638205).

K. Long et al. (Eds.): 5GWN 2017, LNICST 211, pp. 300–316, 2018.
https://doi.org/10.1007/978-3-319-72823-0_29

A receiver that jointly estimates channel taps and data symbols can provide more accurate channel estimation with less pilot overhead [8–11]. Factor graph and loopy belief propagation (LBP) [12] have been used as a unified framework for iterative joint detection, estimation, interference cancellation, and decoding [13]. LBP algorithm combined with various approximate method has been proposed in [9,14–20]. Specifically, LBP combined with expectation-maximization (EM) was proposed in [16]; LBP combined with Gaussian approximation was studied in [9,16,17,21]. Riegler *et al.* merged LBP and the mean-field (MF) approximation (so called "BP-MF") in [19,22], and applied it to both single-input single-output OFDM systems and MIMO-OFDM systems [19,22,23]. However, the BP-MF has to learn the noise precision to take into count the interference from other users even when the noise power is exact known [24,25]. Moreover, the BP-MF in [22] requires high computational complexity and would only work in the case of few antennas and subcarriers, since large matrices need to be inverted to estimate channel coefficients. Although low-complexity BP-MF variants have been presented in [26,27], their performance are degraded.

In this paper, we consider the massive MIMO-OFDM system over frequency selective channels. In order to decouple frequency-domain channel taps and transmit symbols from noisy observations, we use the central-limit theorem to efficiently obtain the joint belief of each pair of frequency-domain channel tap and transmit symbol, and then employ the mean-field method to decouple them. Given messages of frequency-domain channel taps are extracted from observations, the time-domain channel taps between each pair of antennas is estimated by a Gaussian message passing estimator [20]. In addition, the computations at symbol variables are reduced by the expectation propagation [28–30].

The remainder of this paper is organized as follows. The system model is described in Sect. 2. Section 3 presents the proposed message passing algorithm and complexity analysis. Numerical results are presented in Sect. 4, followed by conclusions in Sect. 5.

Notation: Lowercase letters (e.g., x) denote scalars, bold lowercase letters (e.g., $\boldsymbol{x}$) denote column vectors, and bold uppercase letters (e.g., $\boldsymbol{X}$) denote matrices. The superscripts $(\cdot)^{\mathsf{T}}$, $(\cdot)^{\mathsf{H}}$ and $(\cdot)^*$ denote the transpose operation, Hermitian transpose operation, and complex conjugate operation, respectively. Also, $\boldsymbol{X} \otimes \boldsymbol{Y}$ denotes Kronecker product of $\boldsymbol{X}$ and $\boldsymbol{Y}$; $\boldsymbol{I}$ or $\boldsymbol{I}_d$ denotes an identity matrix of size $d \times d$, and $\mathsf{ln}(\cdot)$ denotes the natural logarithm. Furthermore, $\mathcal{N}_{\mathbb{C}}(x; \hat{x}, v_x) = (\pi v_x)^{-1} \mathsf{exp}\left(-|x-\hat{x}|^2 / v_x\right)$ denotes the Gaussian probability density function (PDF) of x with mean $\hat{x}$ and variance v, and $\mathsf{Gam}(\lambda; \alpha, \beta) = \beta^{\alpha} \lambda^{\alpha-1} \mathsf{exp}(-\beta\lambda) / \Gamma(\alpha)$ denotes the Gamma PDF of λ with shape parameter α and rate parameter β, where $\Gamma(\cdot)$ is the gamma function. Finally, $\propto$ denotes equality up to a constant scale factor; $\boldsymbol{x} \backslash x_{tnk}$ denotes all elements in $\boldsymbol{x}$ but x_{tnk}; and $\mathsf{E}_{p(x)} \cdot$ denotes expectation with respect to distribution $p(x)$.

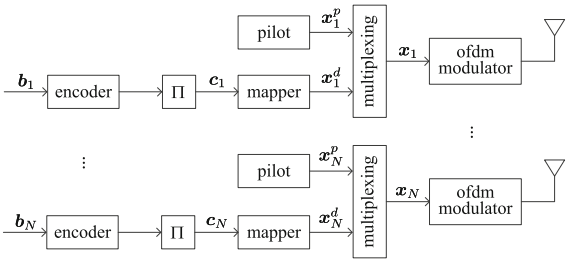

Fig. 1. Block-diagram representation of the transmitters.

2 System Model

We consider the up-link of a massive MIMO system with N users. Each user employs one transmit antenna, and the base station employs an array of $M \geq N$ antennas. Frequency-selective Rayleigh fading channels are assumed, and OFDM is employed to combat multipath interference. The transmitters for the users are shown in Fig. 1. For the nth user, the information bits $\boldsymbol{b}_n$ are encoded and interleaved, yielding a sequence of coded bits $\boldsymbol{c}_n$. Then each Q bits in $\boldsymbol{c}_n$ are mapped onto one modulation symbol, which is chosen from a 2^Q-ary constellation set $\mathcal{A}$, i.e., $|\mathcal{A}| = 2^Q$. The data symbols $\boldsymbol{x}_n^d$ are then multiplexed with pilot symbols $\boldsymbol{x}_n^p$, forming the transmitted symbols sequence $\boldsymbol{x}_n$. Pilot and data symbols are arranged in an OFDM frame of T OFDM symbols, each consisting of K subcarriers. More specifically, there are totally K_p pilot subcarriers in an OFDM frame and the pilot subcarriers are spaced $\lfloor K/(K_p - 1) \rfloor$ subcarriers apart. The pilot-subcarrier set of user n is denoted by $\mathcal{P}_n = \{(t,k) : x_{tnk} \text{ is pilot}\}$, $|\mathcal{P}_n| = T_p K_p$, and data-subcarrier set is denoted by $\mathcal{D} = \overline{\bigcup_n \mathcal{P}_n}$. Note that pilot-subcarrier sets belong to different users are mutual exclusive, i.e., $\bigcap_n \mathcal{P}_n = \emptyset$, and only one user actually transmits a pilot symbol at a given pilot subcarrier, whereas the other users keep silent, i.e., if $(t,k) \in \mathcal{P}_n$, then $x_{tn'k} = 0$, $\forall n' \neq n$. The frequency-domain symbols in the tth OFDM symbol transmitted by the nth user are denoted by $\boldsymbol{x}_{tn} = [x_{tn1}, \ldots, x_{tnK}]^{\mathsf{T}}$, where $x_{tnk} \in \mathcal{A}$ represents the symbol transmitted at the kth subcarrier. To modulate the OFDM symbol, a K-point inverse discrete Fourier transform (IDFT) is applied to the symbol sequence $\boldsymbol{x}_{tn}$, and then a cyclic prefix (CP) is added to it before transmission.

The OFDM symbols are transmitted through a wide-sense stationary uncorrelated scattering (WSSUS) channel. It is assumed that the time-domain channel taps keep static during one OFDM frame but vary from frame to frame. The time-domain channel taps from the nth user to the mth receive antenna are denoted by $\boldsymbol{h}_{mn} = [h_{mn1}, \ldots, h_{mnL}]^{\mathsf{T}}$, where h_{mnl} is the lth channel tap, and L is the maximum number of channel taps. Then, the frequency-domain tap w_{mnk} at the kth subcarrier from the nth user to the mth receiving antenna reads

$$w_{mnk} = \sum_{l=1}^{L} h_{mnl} \exp\left(-\frac{j2\pi lk}{K}\right). \tag{1}$$

At each receive antenna, the CP is first removed and the received signal is then converted into the frequency-domain through a K-point discrete Fourier transform (DFT). It is assumed that the N transmitters and the receiver are synchronized and the maximum delays are smaller than the duration of the CP, whereby the received signal for the tth OFDM symbol can be written as

$$y_{tmk} = \sum_{n=1}^{N} w_{mnk} x_{tnk} + \varpi_{tmk}, \tag{2}$$

where y_{tmk} denotes the received signal at the kth subcarrier on the mth receive antenna, ϖ_{tmk} denotes a circularly symmetric complex noise with zero mean and variance σ_{ϖ}^2. The received signal can be recast in a matrix-vector notation as

$$\boldsymbol{y} = \sum_{n=1}^{N} \boldsymbol{W}_n \boldsymbol{x}_n + \boldsymbol{\varpi} = \boldsymbol{W}\boldsymbol{x} + \boldsymbol{\varpi}, \tag{3}$$

where $\boldsymbol{y} = \left[\boldsymbol{y}_1^{\mathsf{T}} \cdots \boldsymbol{y}_M^{\mathsf{T}}\right]^{\mathsf{T}}$ with $\boldsymbol{y}_m = \left[y_{1m1} \cdots y_{1mK} \cdots y_{Tm1} \cdots y_{TmK}\right]^{\mathsf{T}}$ denoting the received signal at the mth receive antenna for T OFDM symbols, $\boldsymbol{W}_n = \left[\boldsymbol{I}_T \otimes \mathsf{diag}\left\{\boldsymbol{w}_{1n\cdot}\right\} \cdots \boldsymbol{I}_T \otimes \mathsf{diag}\left\{\boldsymbol{w}_{Mn\cdot}\right\}\right]^{\mathsf{T}}$ with $\boldsymbol{w}_{mn\cdot} = \left[w_{mn1} \cdots w_{mnK}\right]^{\mathsf{T}}$ denoting the frequency-domain taps from the nth user to the mth antenna, $\boldsymbol{W} = \left[\boldsymbol{W}_1 \cdots \boldsymbol{W}_N\right]$, $\boldsymbol{x} = \left[\boldsymbol{x}_1^{\mathsf{T}} \cdots \boldsymbol{x}_N^{\mathsf{T}}\right]^{\mathsf{T}}$ with $\boldsymbol{x}_n = \left[x_{1n1} \cdots x_{1nK} \cdots x_{Tn1} \cdots x_{TnK}\right]^{\mathsf{T}}$ denoting the symbols transmitted by the nth user, and $\boldsymbol{\varpi} = \left[\boldsymbol{\varpi}_1^{\mathsf{T}} \cdots \boldsymbol{\varpi}_M^{\mathsf{T}}\right]^{\mathsf{T}}$ with $\boldsymbol{\varpi}_m = \left[\varpi_{1m1} \cdots \varpi_{1mK} \cdots \varpi_{Tm1} \cdots \varpi_{TmK}\right]^{\mathsf{T}}$ denoting the noise signal at the mth receive antenna.

3 Message Passing for Joint Detection and Decoding

We aim to jointly estimate the information bits $\boldsymbol{b} = \left[\boldsymbol{b}_1^{\mathsf{T}} \cdots \boldsymbol{b}_N^{\mathsf{T}}\right]$ and channel taps $\boldsymbol{h} = \left[\boldsymbol{h}_{11\cdot}^{\mathsf{T}} \cdots \boldsymbol{h}_{1N\cdot}^{\mathsf{T}} \cdots \boldsymbol{h}_{M1\cdot}^{\mathsf{T}} \cdots \boldsymbol{h}_{MN\cdot}^{\mathsf{T}}\right]^{\mathsf{T}}$ from the noisy observation $\boldsymbol{y}$. The joint PDF of all involved random variables can be factorized as follows,

$$\begin{aligned}
&p\left(\boldsymbol{b}, \boldsymbol{c}, \boldsymbol{x}, \boldsymbol{y}, \boldsymbol{W}, \boldsymbol{h}\right) \\
&\quad = p\left(\boldsymbol{b}\right) p\left(\boldsymbol{c} \mid \boldsymbol{b}\right) p\left(\boldsymbol{x} \mid \boldsymbol{c}\right) p\left(\boldsymbol{y} \mid \boldsymbol{W}, \boldsymbol{x}\right) p\left(\boldsymbol{h}, \boldsymbol{W}\right) \\
&\quad = p\left(\boldsymbol{b}\right) p\left(\boldsymbol{c} \mid \boldsymbol{b}\right) \prod_{n=1}^{N} \prod_{(t,k)\in\mathcal{D}} \mathcal{M}_{tnk}\left(x_{tnk}, \boldsymbol{c}_{tnk}\right) \prod_{t,m,k} f_{tmk}\left(\boldsymbol{x}_{t\cdot k}, \boldsymbol{w}_{tmk}\right) \\
&\qquad \times \prod_{m,n,k} g_{mnk}\left(w_{mnk}, \boldsymbol{h}_{mn\cdot}\right) \prod_{m,n,l} p\left(h_{mnl}\right),
\end{aligned} \tag{4}$$

where $\mathcal{M}_{tnk}\left(x_{tnk}, \boldsymbol{c}_{tnk}\right) = \delta\left(\varphi\left(\boldsymbol{c}_{tnk}\right) - x_{tnk}\right)$ denotes the deterministic mapping $x_{tnk} = \varphi\left(\boldsymbol{c}_{tnk}\right)$, $\varphi\left(\boldsymbol{c}_{tnk}\right)$ denotes the symbol mapping function, and $\delta\left(\cdot\right)$ denotes the Kronecker delta function. The channel transition function $f_{tmk}(\boldsymbol{x}_{t\cdot k}, \boldsymbol{w}_{mnk})$ is given by

$$f_{tmk}(\boldsymbol{x}_{t\cdot k}, \boldsymbol{w}_{mnk}) = \mathcal{N}_{\mathbb{C}}\left(y_{tmk}; \sum_{n} w_{mnk} x_{mnk}, \sigma_{\varpi}^2\right). \tag{5}$$

As the frequency-domain channel taps w_{mnk} is the DFT (discrete Fourier transform) of time-domain taps $\boldsymbol{h}_{mn\cdot}$, we have

$$g_{mnk}\left(w_{mnk}, \boldsymbol{h}_{mn\cdot}\right) = \delta\left(w_{mnk} - \sum_{l=1}^{L} \phi_{kl} h_{mnl}\right), \tag{6}$$

where $\boldsymbol{\Phi} \in \mathbb{C}^{K \times L}$ denotes the DFT weighting matrix, and ϕ_{kl} denotes the entry in the kth row and lth column of DFT weighting matrix $\boldsymbol{\Phi}$. The probabilistic structure exposed by the factorization (4) can be represented with a factor graph, as depicted in Fig. 2. Due to high-dimensional integration, directly computing the marginal probability of information bit is computationally prohibitive. Hence, we resort to LBP to offer efficient solutions. As shown in Fig. 2, there exist two groups of loops, the group of detection-decoding-loops in the left and the group of the channel-estimation-loops in the right. Here, we choose to start passing messages at the channel transition nodes, then pass messages concurrently in both the detection-decoding-loop (the left loop) and the channel-estimation-loop (the right loop). Each of these full cycles of message passing will be referred to as a "turbo iteration".

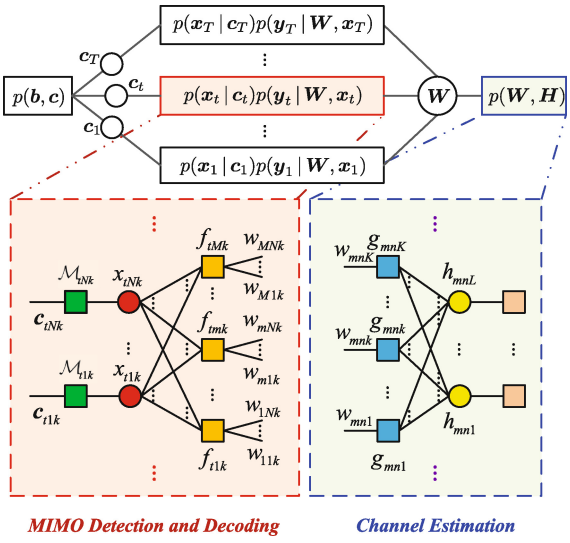

Fig. 2. Factor graph of the Massive MIMO-OFDM system.

The presentation of message passing follows closely with the convention in [12]. All types of message are specified in Table 1. Applying the SPA to the factor graph in Fig. 2, the messages from the channel transition node f_{tmk} at the ith iteration are given by

Table 1. SPA message definitions at iteration $i \in \mathbb{Z}$.

$\mu^{(i)}_{tnk\leftarrow tmk}(\cdot)$	Message from node f_{tmk} to node x_{tnk}
$\mu^{(i)}_{tnk\leftarrow tnk}(\cdot)$	Message from node x_{tnk} to node $\mathcal{M}_{tnk}$
$\mu^{(i)}_{tnk\rightarrow tnk}(\cdot)$	Message from node $\mathcal{M}_{tnk}$ to node x_{tnk}
$\mu^{(i)}_{tnk\rightarrow tmk}(\cdot)$	Message from node x_{tnk} to node f_{tmk}
$\mu^{(i)}_{tmk\rightarrow mnk}(\cdot)$	Message from node f_{tmk} to node w_{mnk}
$\mu^{(i)}_{mnk\rightarrow mnk}(\cdot)$	Message from node w_{mnk} to node g_{mnk}
$\mu^{(i)}_{mnk\rightarrow mnl}(\cdot)$	Message from node g_{mnk} to node h_{mnl}
$\mu^{(i)}_{mnl\rightarrow mnk}(\cdot)$	Message from node h_{mnl} to node g_{mnk}
$\mu^{(i)}_{mnk\leftarrow mnk}(\cdot)$	Message from node g_{mnk} to node w_{mnk}
$\mu^{(i)}_{tmk\leftarrow mnk}(\cdot)$	Message from node w_{mnk} to node f_{tmk}
$\beta^{(i)}_{tnk}(\cdot)$	Belief of x_{tnk} at node x_{tnk}
$\beta^{(i)}_{mnk}(\cdot)$	Belief of w_{mnk} at node w_{mnk}

$$\mu^{(i)}_{tnk\leftarrow tmk}(x_{tnk}) = \sum_{\boldsymbol{x}_{t\cdot k}\backslash x_{tnk}} \int_{\boldsymbol{w}_{mk}} \Bigg(f_{tmk}(\boldsymbol{x}_{t\cdot k}, \boldsymbol{w}_{m\cdot k}) \times \prod_{n'=1}^{N} \mu^{(i-1)}_{tmk\leftarrow mn'k}(w_{mn'k}) \prod_{n''\neq n}^{N} \mu^{(i-1)}_{tn''k\rightarrow tmk}(x_{tn''k}) \Bigg), \forall n, \tag{7}$$

$$\mu^{(i)}_{tmk\rightarrow mnk}(w_{mnk}) = \sum_{\boldsymbol{x}_{t\cdot k}\in\mathcal{A}^N} \int_{\boldsymbol{w}_{m\cdot k}\backslash w_{mnk}} \Bigg(f_{tmk}(\boldsymbol{x}_{t\cdot k}, \boldsymbol{w}_{m\cdot k}) \times \prod_{n'\neq n} \mu^{(i-1)}_{tmk\leftarrow mn'k}(w_{mn'k}) \prod_{n''} \mu^{(i-1)}_{tn''k\rightarrow tmk}(x_{tn''k}) \Bigg), \forall n. \tag{8}$$

As each symbol of $\boldsymbol{x}_{t\cdot k}\backslash x_{tnk} \in \mathcal{A}^{N-1}$ takes on values in the discrete set $\mathcal{A}$, the computations of $\mu^{(i)}_{tnk\leftarrow tmk}(x_{tnk})$ and $\mu^{(i)}_{tmk\rightarrow mnk}(w_{mnk})$ require exponential time to marginalize out the random vector $\boldsymbol{x}_{t\cdot k}\backslash x_{tnk}$, which are obviously intractable for the problem size of interests. Using (5), the messages with respect to known pilot symbol boil down to the following simple form

$$\mu^{(i)}_{tmk\rightarrow mnk}(w_{mnk}) \propto \mathcal{N}_{\mathbb{C}}\left(w_{mnk}; \frac{y_{tmk}}{x_{tnk}}, \frac{\sigma^2_{\varpi}}{|x_{tnk}|^2}\right), \forall (t,k) \in \mathcal{P}_n \tag{9}$$

$$\mu^{(i)}_{tmk\rightarrow mn'k}(w_{mn'k}) \propto \mathcal{N}_{\mathbb{C}}(w_{mn'k}; 0, \infty), \forall n' \neq n, \tag{10}$$

where we make use of the fact that other users keep silent on the pilot subcarriers $\mathcal{P}_n$.

3.1 LBP Combined with Gaussian Approximation and Mean-Field Approximation

Note that, to update the outgoing messages from the observation node f_{tmk}, the received signal in (2) can be rewritten as

$$y_{tmk} = w_{mnk}x_{tnk} + \sum_{n' \neq n}^{N} w_{mn'k}x_{tn'k} + \varpi_{tmk}, \forall n. \tag{11}$$

The interference term $\sum_{n' \neq n} w_{mn'k}x_{tn'k} + \varpi_{tmk}$ in (11) is considered as a Gaussian variable with mean $\tilde{z}^{(i)}_{tnk \leftarrow tmk}$ and variance $\tau^{(i)}_{tnk \leftarrow tmk}$,

$$\begin{aligned}
\tilde{z}^{(i)}_{tnk \leftarrow tmk} &= \sum_{n' \neq n} \hat{w}^{(i-1)}_{tmk \leftarrow mn'k} \hat{x}^{(i-1)}_{tn'k \rightarrow tmk}, \\
\tau^{(i)}_{tnk \leftarrow tmk} &= \sigma^2_{\varpi} + \sum_{n' \neq n} \Big(\big|\hat{w}^{(i-1)}_{tmk \leftarrow mn'k}\big|^2 \nu^{(i-1)}_{tn'k \rightarrow tmk} \\
&\quad + \big|\hat{x}^{(i-1)}_{tn'k \rightarrow tmk}\big|^2 \nu^{(i-1)}_{tmk \leftarrow mn'k} + \nu^{(i-1)}_{tn'k \rightarrow tmk} \nu^{(i-1)}_{tmk \leftarrow mn'k} \Big).
\end{aligned} \tag{12}$$

where $\hat{w}^{(i-1)}_{tmk \leftarrow mn'k}$ and $\nu^{(i-1)}_{tmk \leftarrow mn'k}$ denote the mean and variance of variable x_{tnk} with respect to the message $\mu^{(i-1)}_{tmk \leftarrow mn'k}(w_{mnk})$, respectively; $\hat{x}^{(i-1)}_{tn'k \rightarrow tmk}$ and $\nu^{(i-1)}_{tn'k \rightarrow tmk}$ denote the mean and variance of variable w_{mnk} with respect to message $\mu^{(i-1)}_{tn'k \rightarrow tmk}(x_{tnk})$, respectively. As a result, the channel transition function f_{tmk} can be approximated as

$$f_{tmk}(\boldsymbol{x}_{t \cdot k}, \boldsymbol{w}^k_m) \approx \mathcal{N}_{\mathbb{C}}(w_{mnk}x_{tnk}; z^{(i)}_{tmk \rightarrow mnk}, \tau^{(i)}_{tmk \rightarrow mnk}), \forall n, \tag{13}$$

where $z^{(i)}_{tmk \rightarrow mnk} = y_{tmk} - \tilde{z}^{(i)}_{tnk \leftarrow tmk}$.

Using (13), a local joint belief of w_{mnk} and x_{tnk} is defined as

$$\begin{aligned}
\beta^{(i)}_{tmk}(w_{mnk}, x_{tnk}) \propto \mathcal{N}_{\mathbb{C}}(x_{tnk}w_{mnk}; z^{(i)}_{tmk \rightarrow mnk}, \tau^{(i)}_{tmk \rightarrow mnk}) \\
\times \mu^{(i-1)}_{tmk \leftarrow mnk}(w_{mnk}) \mu^{(i-1)}_{tnk \rightarrow tmk}(x_{tnk}),
\end{aligned} \tag{14}$$

In order to maintain the message passing analytically and efficiently, we project the joint belief $\beta^{(i)}_{tmk}(w_{mnk}, x_{tnk})$ onto a fully factorized belief $\tilde{\beta}^{(i)}_{tmk}(w_{mnk}, x_{tnk}) = \tilde{\beta}^{(i)}_{tmk}(x_{tnk})\,\tilde{\beta}^{(i)}_{tmk}(w_{mnk})$, using the criterion of minimum inclusive KL divergence [31]

$$\min_{\tilde{\beta}^{(i)}_{tmk}(w_{mnk}, x_{tnk})} \mathrm{KL}\left(\tilde{\beta}^{(i)}_{tmk}(w_{mnk}, x_{tnk}) \parallel \beta^{(i)}_{tmk}(w_{mnk}, x_{tnk}) \right), \tag{15}$$

which amounts to the mean-field approximation in statistical physics. However, finding a global optimal solution to (15) is difficult, and hence, we instead resort to a local form of optimization. We use alternative measures to find the local beliefs $\tilde{\beta}^{(i)}_{tmk}(x_{tnk})$ and $\tilde{\beta}^{(i)}_{tmk}(w_{mnk})$ at the function node f_{tmk}

$$\mathsf{KL}\left(\tilde{\beta}_{tmk}^{(i)}\left(x_{tnk}\right)\tilde{\beta}_{tmk}^{(i-1)}\left(w_{mnk}\right)\parallel\beta_{tmk}^{(i)}\left(w_{mnk},x_{tnk}\right)\right), \tag{16}$$

$$\mathsf{KL}\left(\tilde{\beta}_{tmk}^{(i)}\left(w_{mnk}\right)\tilde{\beta}_{tmk}^{(i-1)}\left(x_{tnk}\right)\parallel\beta_{tmk}^{(i)}\left(w_{mnk},x_{tnk}\right)\right), \tag{17}$$

where the local beliefs $\tilde{\beta}_{tmk}^{(i-1)}\left(w_{mnk}\right)$ and $\tilde{\beta}_{tmk}^{(i-1)}\left(x_{tnk}\right)$ at variable nodes x_{tnk} and w_{mnk}, respectively, are defined later. Using variational calculus, $\tilde{\beta}_{tmk}^{(i)}\left(x_{tnk}\right)$ and $\tilde{\beta}_{tmk}^{(i)}\left(w_{mnk}\right)$ fulfill following updates[1]

$$\tilde{\beta}_{tmk}^{(i)}\left(x_{tnk}\right)=\exp\left(\mathsf{E}_{\beta_{mnk}^{(i-1)}\left(w_{mnk}\right)}\ln\beta_{tmk}^{(i)}\left(w_{mnk},x_{tnk}\right)\right), \tag{18}$$

$$\tilde{\beta}_{tmk}^{(i)}\left(w_{mnk}\right)=\exp\left(\mathsf{E}_{\beta_{tnk}^{(i-1)}\left(x_{tnk}\right)}\ln\beta_{tmk}^{(i)}\left(w_{mnk},x_{tnk}\right)\right). \tag{19}$$

According to the semantics of factor graph, the messages $\mu_{tnk\leftarrow tmk}^{(i)}\left(x_{tnk}\right),\forall n$ and $\mu_{tmk\rightarrow mnk}^{(i)}\left(w_{mnk}\right),\forall n$ then are updated as follows

$$\begin{aligned}\mu_{tnk\leftarrow tmk}^{(i)}\left(x_{tnk}\right)&=\frac{\tilde{\beta}_{tmk}^{(i)}\left(x_{tnk}\right)}{\mu_{tnk\rightarrow tmk}^{(i-1)}\left(x_{tnk}\right)}\propto\mathcal{N}_{\mathbb{C}}\left(x_{tnk};\hat{x}_{tnk\leftarrow tmk}^{(i)},\nu_{tnk\leftarrow tmk}^{(i)}\right),\\ \mu_{tmk\rightarrow mnk}^{(i)}\left(w_{mnk}\right)&=\frac{\tilde{\beta}_{tmk}^{(i)}\left(w_{mnk}\right)}{\mu_{tmk\leftarrow mnk}^{(i-1)}\left(w_{mnk}\right)}\propto\mathcal{N}_{\mathbb{C}}\left(w_{mnk};\hat{w}_{tmk\rightarrow mnk}^{(i)},\nu_{tmk\rightarrow mnk}^{(i)}\right),\end{aligned} \tag{20}$$

where

$$\nu_{tnk\leftarrow tmk}^{(i)}=\frac{\tau_{tmk\rightarrow mnk}^{(i)}}{\nu_{mnk}^{(i-1)}+\left|\hat{w}_{mnk}^{(i-1)}\right|^{2}}, \tag{21}$$

$$\hat{x}_{tnk\leftarrow tmk}^{(i)}=\frac{\nu_{tnk\leftarrow tmk}^{(i)}}{\tau_{tmk\rightarrow mnk}^{(i)}}\hat{w}_{mnk}^{(i-1)*}z_{tnk\leftarrow tmk}^{(i)}, \tag{22}$$

$$\nu_{tmk\rightarrow mnk}^{(i)}=\frac{\tau_{tmk\rightarrow mnk}^{(i)}}{\nu_{tnk}^{(i-1)}+\left|\hat{x}_{tnk}^{(i-1)}\right|^{2}}, \tag{23}$$

$$\hat{w}_{tmk\rightarrow mnk}^{(i)}=\frac{\nu_{tmk\rightarrow mnk}^{(i)}}{\tau_{tmk\rightarrow mnk}^{(i)}}\hat{x}_{tnk}^{(i-1)*}z_{tmk\rightarrow mnk}^{(i)}. \tag{24}$$

with $z_{tnk\leftarrow tmk}^{(i)}$ and $\tau_{tmk\rightarrow mnk}^{(i)}$ having the same definitions as that of (12) and (12), respectively. Next, the local belief at the variable node x_{tnk} is updated by

[1] For the sake of efficient implementation, we consider to update all the beliefs concurrently in this paper.

$$\beta_{tnk}^{(i)}\left(x_{tnk}\right)=\frac{\mu_{tnk\to tnk}^{(i)}\left(x_{tnk}\right)\prod_m\mu_{tnk\leftarrow tmk}^{(i)}\left(x_{tnk}\right)}{\sum_{x_{tnk}\in\mathcal{A}}\mu_{tnk\to tnk}^{(i)}\left(x_{tnk}\right)\prod_m\mu_{tnk\leftarrow tmk}^{(i)}\left(x_{tnk}\right)}$$
$$=\frac{\mu_{tnk\to tnk}^{(i)}\left(x_{tnk}\right)\mathcal{N}_{\mathbb{C}}(x_{tnk};\zeta_{tnk}^{(i)},\gamma_{tnk}^{(i)})}{\sum_{x_{tnk}\in\mathcal{A}}\mu_{tnk\to tnk}^{(i)}\left(x_{tnk}\right)\mathcal{N}_{\mathbb{C}}(x_{tnk};\zeta_{tnk}^{(i)},\gamma_{tnk}^{(i)})},\tag{25}$$

where

$$\gamma_{tnk}^{(i)}=\frac{1}{\sum_{m=1}^{M}\frac{1}{\nu_{tnk\leftarrow tmk}^{(i)}}},\tag{26}$$

$$\zeta_{tnk}^{(i)}=\gamma_{tnk}^{(i)}\sum_{m=1}^{M}\frac{\hat{x}_{tnk\leftarrow tmk}^{(i)}}{\nu_{tnk\leftarrow tmk}^{(i)}}.\tag{27}$$

Then the message $\mu_{tnk\leftarrow tnk}^{(i)}\left(x_{tnk}\right)$ from the variable node x_{tnk} to the mapper node $\mathcal{M}_{tnk}$ is updated by

$$\mu_{tnk\leftarrow tnk}^{(i)}\left(x_{tnk}\right)=\prod_{m=1}^{M}\mu_{tnk\leftarrow tmk}^{(i)}\left(x_{tnk}\right)\propto\mathcal{N}_{\mathbb{C}}\left(x_{tnk};\zeta_{tnk}^{(i)},\gamma_{tnk}^{(i)}\right).\tag{28}$$

With the message $\mu_{tnk\leftarrow tnk}^{(i)}\left(x_{tnk}\right)$ and the *a priori* LLRs $\left\{\lambda_{\mathsf{a}}^{(i-1)}\left(c_{tnk}^{q}\right),\forall q\right\}$ fed from decoder, the extrinsic LLRs $\{\lambda_{\mathsf{e}}^{(i)}\left(c_{tnk}^{q}\right),\forall q\}$ corresponding to the symbol x_{tnk} are obtained

$$\lambda_{\mathsf{e}}^{(i)}\left(c_{tnk}^{q}\right)=\mathsf{ln}\frac{\sum_{x_{tnk}\in\mathcal{A}_q^1}\mu_{tnk\to tnk}^{(i-1)}\left(x_{tnk}\right)\mu_{tnk\leftarrow tnk}^{(i)}\left(x_{tnk}\right)}{\sum_{x_{tnk}\in\mathcal{A}_q^0}\mu_{tnk\to tnk}^{(i-1)}\left(x_{tnk}\right)\mu_{tnk\leftarrow tnk}^{(i)}\left(x_{tnk}\right)}-\lambda_{\mathsf{a}}^{(i-1)}\left(c_{tnk}^{q}\right).\tag{29}$$

Once all the extrinsic LLRs $\{\lambda_{\mathsf{e}}^{(i)}\left(c_{tnk}^{q}\right),\forall t,\forall n,\forall k,\forall q\}$ are available, each channel decoder performs decoding and updates the *a priori* LLRs of coded bits. Then, the *a priori* LLRs $\left\{\lambda_{\mathsf{a}}^{(i)}\left(c_{tnk}^{q}\right)\right\}$ are interleaved and converted to the message

$$\mu_{tnk\to tnk}^{(i)}\left(x_{tnk}\right)=\prod_{q=1}^{Q}\frac{\mathsf{exp}\left(c_n^q\lambda_{\mathsf{a}}^{(i)}\left(c_{tnk}^{q}\right)\right)}{1+\mathsf{exp}\left(\lambda_{\mathsf{a}}^{(i)}\left(c_{tnk}^{q}\right)\right)}.\tag{30}$$

Direct evaluating $\left\{\hat{x}_{tnk\to tmk}^{(i)},\nu_{tnk\to tmk}^{(i)}\right\}$ via $\mu_{tnk\to tmk}^{(i)}\left(x_{tnk}\right)$ is expensive, as the number of $\left\{\hat{x}_{tnk\to tmk}^{(i)},\nu_{tnk\to tmk}^{(i)},\forall t,\forall m,\forall n\right\}$ is up to TMN. Following the expectation propagation method proposed in [28], we can reduce the computational complexity of $\left\{\hat{\mu}_{tnk\to tmk}^{(i)}\left(x_{tnk}\right)\right\}$. We consider every transmitted symbol x_{tnk} as a continuous random variable and will approximate its message $\mu_{tnk\to tmk}^{(i)}\left(x_{tnk}\right)$ as a complex Gaussian PDF $\hat{\mu}_{tnk\to tmk}^{(i)}\left(x_{tnk}\right)=\mathcal{N}_{\mathbb{C}}\left(x_{tnk};\hat{x}_{tnk\to tmk}^{(i)},\nu_{tnk\to tmk}^{(i)}\right)$.

The symbol belief $\beta_{tnk}^{(i)}(x_{tnk})$ at the variable node is projected into a Gaussian PDF denoted by $\hat{\beta}_n^{(i)}(x_{tnk}) = \mathcal{N}_{\mathbb{C}}\left(x_{tnk}; \hat{x}_{tnk}^{(i)}, \nu_{tnk}^{(i)}\right)$, where

$$\hat{x}_{tnk}^{(i)} = \sum_{\alpha_s \in \mathcal{A}} \alpha_s \beta_{tnk}^{(i)}(x_{tnk} = \alpha_s), \tag{31}$$

$$\nu_{tnk}^{(i)} = \sum_{\alpha_s \in \mathcal{A}} |\alpha_s|^2 \beta_{tnk}^{(i)}(x_{tnk} = \alpha_s) - \left|\hat{x}_{tnk}^{(i)}\right|^2. \tag{32}$$

Then the approximate message $\hat{\mu}_{tnk\to tmk}^{(i)}(x_{tnk})$ is computed from the approximate symbol belief $\hat{\beta}_n^{(i)}(x_{tnk})$ as following

$$\hat{\mu}_{tnk\to tmk}^{(i)}(x_{tnk}) \approx \frac{\hat{\beta}_n^{(i)}(x_{tnk})}{\mu_{tnk\leftarrow tmk}^{(i)}(x_{tnk})} \propto \mathcal{N}_{\mathbb{C}}(x_{tnk}; \hat{x}_{tnk\to tmk}^{(i)}, \nu_{tnk\to tmk}^{(i)}), \tag{33}$$

where

$$\hat{x}_{tnk\to tmk}^{(i)} = \hat{x}_{tnk}^{(i)} + \nu_{tnk}^{(i)} \frac{\hat{x}_{tnk}^{(i)} - \hat{x}_{tnk\leftarrow tmk}^{(i)}}{\nu_{tnk\leftarrow tmk}^{(i)} - \nu_{tnk}^{(i)}}, \tag{34}$$

$$\nu_{tnk\to tmk}^{(i)} = \frac{\nu_{tnk}^{(i)} \nu_{tnk\leftarrow tmk}^{(i)}}{\nu_{tnk\leftarrow tmk}^{(i)} - \nu_{tnk}^{(i)}}. \tag{35}$$

We will refer to the proposed message passing as "BP-GMF", which is be summarized in Algorithm 1.

3.2 Complexity Comparisons

Table 2 shows the proposed scheme and other message-passing schemes. The computationally complexity of these scheme is compared in terms of floating-point operations (FLOPs) per iteration. For simplicity, the complexity of addition, subtraction, multiplication, and division is considered as being identical. Furthermore, we don't take the operations of $\exp(\cdot)$ and $\left\{\lambda_e^{(i)}(c_{tnk}^q)\right\}$ into accounted. Table 3 shows that the complexity of BP-MF-GMP, BP-GMF and BP-MF is $\mathcal{O}(T(M + Q|\mathcal{A}|)NK)$, and that of BP-GA is

Table 2. Receiver schemes and their component algorithms.

Receiver scheme	Channel estimation	Detection & decoding
BP-GA	GMP	BP-GA [32]
BP-GMF	GMP	BP-GMF
BP-MF	Algorithm in [22] using disjoint channel model	BP-MF [19,22]
BP-MF-M	Algorithm in [26] using markov channel model	BP-MF [19,22]
BP-MF-GAMP	GAMP	BP-MF [27]

Algorithm 1. The BP-GMF algorithm at the ith turbo iteration.

Initialization: $\hat{w}_{mnk\to tmk}^{(0)}=0, \nu_{mnk\to tmk}^{(0)}=, \forall k, \forall l.$

for t, n, k, m **do**

$z_{tnk\leftarrow tmk}^{(i)}=\sum_{n'\neq n}\hat{w}_{tmk\leftarrow mn'}^{(i-1)}\hat{x}_{tn'k\to tmk}^{(i-1)};$

$\tau_{tnk\leftarrow tmk}^{(i)}=\sigma_{\varpi}^{2}+\sum_{n'\neq n}\left[\left|\hat{w}_{tmk\leftarrow mn'}^{(i-1)}\right|^{2}\nu_{tn'k\to tmk}^{(i-1)}+\left(\left|\hat{x}_{tn'k\to tmk}^{(i-1)}\right|^{2}+\nu_{tn'k\to tmk}^{(i-1)}\right)\nu_{tmk\leftarrow mn'}^{(i-1)}\right]$

$\nu_{tnk\leftarrow tmk}^{(i)}=\frac{\tau_{tnk\leftarrow tmk}^{(i)}}{\left|\hat{w}_{mnk}^{(i-1)}\right|^{2}+\nu_{mnk}^{(i-1)}}\quad \nu_{tmk\to mnk}^{(i)}=\frac{\tau_{tnk\leftarrow tmk}^{(i)}}{\left|\hat{x}_{tnk}^{(i-1)}\right|^{2}+\nu_{tnk}^{(i)}};$

$\hat{x}_{tnk\leftarrow tmk}^{(i)}=\nu_{tnk\leftarrow tmk}^{(i)}\left(\hat{w}_{mn}^{(i-1)}\right)^{*}z_{tnk\leftarrow tmk}^{(i)}/\tau_{tnk\leftarrow tmk}^{(i)};$

$\hat{w}_{tmk\to mnk}^{(i)}=\nu_{tnk\leftarrow tmk}^{(i)}\left(\hat{x}_{tnk}^{(i-1)}\right)^{*}z_{tnk\leftarrow tmk}^{(i)}/\tau_{tnk\leftarrow tmk}^{(i)};$

end for

for t, n, k **do**

$\gamma_{tnk}^{(i)}=\left(\sum_{m}1/\nu_{tnk\leftarrow tmk}^{(i)}\right)^{-1};$

$\zeta_{tnk}^{(i)}=\gamma_{tnk}^{(i)}\sum_{m}\left(\hat{x}_{tnk\leftarrow tmk}^{(i)}/\nu_{tnk\leftarrow tmk}^{(i)}\right);$

$\tilde{p}_{eq}^{(i)}\left(x_i\right)=\mu_{tnk\to tnk}^{(i-1)}\left(x_{tnk}\right)\mathcal{N}_{\mathbb{C}}\left(x_{tnk};\zeta_{tnk}^{(i)},\gamma_{tnk}^{(i)}\right);$

$\lambda_{e}^{(i)}\left(c_{tnk}^{q}\right)=\ln\frac{\sum_{x_{tnk}\in\mathcal{A}_{q}^{1}}\tilde{p}_{eq}^{(i)}\left(x_i\right)}{\sum_{x_{tnk}\in\mathcal{A}_{q}^{0}}\tilde{p}_{eq}^{(i)}\left(x_i\right)}-\lambda_{a}^{(i-1)}\left(c_{tnk}^{q}\right).$

end for

for n **do**

Decode and generate LLRs $\{\lambda_{a}^{(i)}\left(c_{tnk}^{q}\right),\forall t,\forall k,\forall q\};$

end for

for t, n, k **do**

$\mu_{tnk\to tnk}^{(i)}\left(x_{tnk}\right)=\prod_{q}\exp\left(c_{tnk}^{q}\lambda_{a}^{(i)}\left(c_{tnk}^{q}\right)\right)/\left(1+\exp\left(\lambda_{a}^{(i)}\left(c_{tnk}^{q}\right)\right)\right);$

$\beta_{tnk}^{(i)}\left(x_{tnk}\right)=\frac{\mu_{tnk\to tnk}^{(i)}\left(x_{tnk}\right)\mathcal{N}_{\mathbb{C}}\left(x_{tnk};\zeta_{tnk}^{(i)},\gamma_{tnk}^{(i)}\right)}{\sum_{x_{tnk}\in\mathcal{A}}\mu_{tnk\to tnk}^{(i)}\left(x_{tnk}\right)\mathcal{N}_{\mathbb{C}}\left(x_{tnk};\zeta_{tnk}^{(i)},\gamma_{tnk}^{(i)}\right)};$

$\hat{x}_{tnk}^{(i)}=\sum_{\alpha_s\in\mathcal{A}}\alpha_s\beta_{tnk}^{(i)}(x_{tnk}=\alpha_s);$

$\nu_{tnk}^{(i)}=\sum_{\alpha_s\in\mathcal{A}}|\alpha_s|^{2}\beta_{tnk}^{(i)}(x_{tnk}=\alpha_s)-|\hat{x}_{tnk}^{(i)}|^{2}.$

$\nu_{tnk\to tmk}^{(i)}=\nu_{tnk}^{(i)}\nu_{tnk\leftarrow tmk}^{(i)}/(\nu_{tnk\leftarrow tmk}^{(i)}-\nu_{tnk}^{(i)}),\forall m;$

$\hat{x}_{tnk\to tmk}^{(i)}=\hat{x}_{tnk}^{(i)}+\nu_{tnk}^{(i)}(\hat{x}_{tnk}^{(i)}-\hat{x}_{tnk\leftarrow tmk}^{(i)})/(\nu_{tnk\leftarrow tmk}^{(i)}-\nu_{tnk}^{(i)}),\forall m.$

end for

Table 3. Complexity of detection and decoding.

Receiver scheme	FLOPs per iteration
BP-GA	$(28\left\|\mathcal{A}\right\|+33)TMNK+(2\left\|\mathcal{A}\right\|+3Q\left\|\mathcal{A}\right\|+Q)TNK$
BP-GMF	$63TMNK+(23\left\|\mathcal{A}\right\|+3Q\left\|\mathcal{A}\right\|+Q)TNK$
BP-MF [22]	$22TMNK+(11N+4)M(K-K_{\mathsf{p}})+(23\left\|\mathcal{A}\right\|+3Q\left\|\mathcal{A}\right\|+Q)TNK$
BP-MF-M [26]	$33TMNK+(11N+4)M(K-K_{\mathsf{p}})+(23\left\|\mathcal{A}\right\|+3Q\left\|\mathcal{A}\right\|+Q)TNK$
BP-MF-GMP	$33TMNK+(11N+4)M(K-K_{\mathsf{p}})+(23\left\|\mathcal{A}\right\|+3Q\left\|\mathcal{A}\right\|+Q)TNK$

$\mathcal{O}\left(T(M\left|\mathcal{A}\right|+Q\left|\mathcal{A}\right|)NK\right)$. Table 4 shows the complexity of algorithms performing the task of channel estimation, where GMP is $\mathcal{O}\left(MNK\left(\log_2 K+T\right)\right)$, BP-MF is $\mathcal{O}\left(MNK^3\right)$, and BP-MF-M is $\mathcal{O}\left(MNKG^3\right)$.

Table 4. Complexity of channel estimation.

Receiver scheme	FLOPs per iteration
BP-GA	$MN\left(20K\log_2 K + 30TK + 11K - 26TK_p + 13K_p + 14L - 2\right)$
BP-GMF	
BP-MF-GAMP [27]	
BP-MF [22]	$MN\left(16K^3 + 12K^2 + 17TK - K\right) + 2TNK - 2NK - 2MN$
BP-MF-M [26]	$MN\left(118G^2 + 68G - 4\right)K - 112G^3 - 92G^3 + 5G$

4 Simulation Results

The proposed receiver algorithm BP-GMF is compared with the BP-GA [32], BP-MF variants, the MMSE, and the MFB-PCSI in terms of bit error rate (BER) and mean square error (MSE) of the channel estimation. A MIMO system with $N = 8$ single-antenna users is considered, each of which employs an OFDM with $K = 64$ subcarriers. We choose a $R = 1/2$ recursive systematic convolutional (RSC) code with generator polynomial $[G_1, G_2] = [117, 155]_{\mathsf{oct}}$, followed by a random interleaver. For bit-to-symbol mapping, multilevel Gray-mapping is used. Each user employs $K_p = 8$ pilot subcarriers modulated with uniformly selected known BPSK symbols and uniformly placed in one selected OFDM symbol. The channel model in simulations is an 8-tap Rayleigh fading MIMO channel with equal tap power. At the receiver, the BCJR algorithm is used to decode the convolutional code. It is assumed that the transmit antennas from different users are spatially uncorrelated and that the receive antenna spacing is sufficient so that they are also spatially uncorrelated. The channels are block-static for the selected 8 transmitted OFDM symbols. For all simulation results, a minimum of 100 frame errors were counted. The energy per bit to noise power spectral density ratio E_b/N_0 is defined as [33]

$$\frac{E_b}{N_0} = \frac{E_s}{N_0} + 10\log_{10}\frac{M}{RNQ}, \tag{36}$$

where E_s/N is the average energy per transmitted symbol.

4.1 Channel-Tap NMSE Versus E_b/N_0

At the initial turbo iteration, only the pilots can be used for channel estimation. The BP-GMF, the BP-GA and the BP-MF-GAMP perform 5 inner iterations in the channel-estimation-loops during the initial turbo iteration and perform only 1 inner iteration during each subsequent turbo iterations. The channel estimator in the BP-MF is equivalent to the pilot-based LMMSE estimator at the initial turbo iteration and becomes the data-aided LMMSE estimator at subsequent turbo iterations. The channel estimation in the BP-MF-M is performed by the Kalman smoother proposed in [26], where the group-size of contiguous channel weights is set to $G = 4$. A maximum of 50 turbo iterations are used in all message-passing receivers, and the NMSE at the ith turbo iteration is calculated by

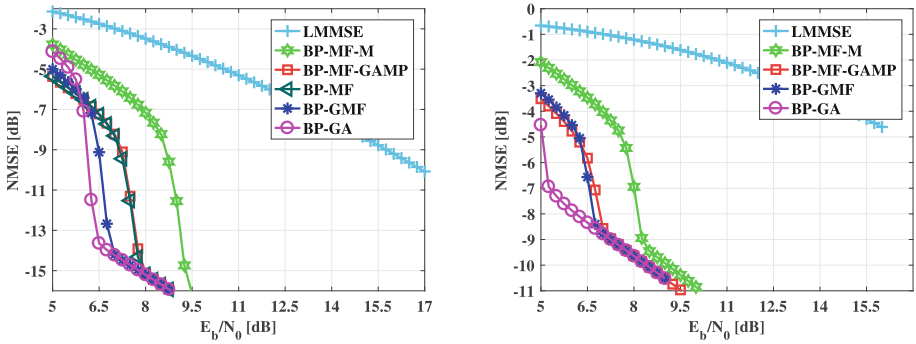

(a) 16×8 (b) 64×8

Fig. 3. NMSE of time-domain channel taps versus E_b/N_0.

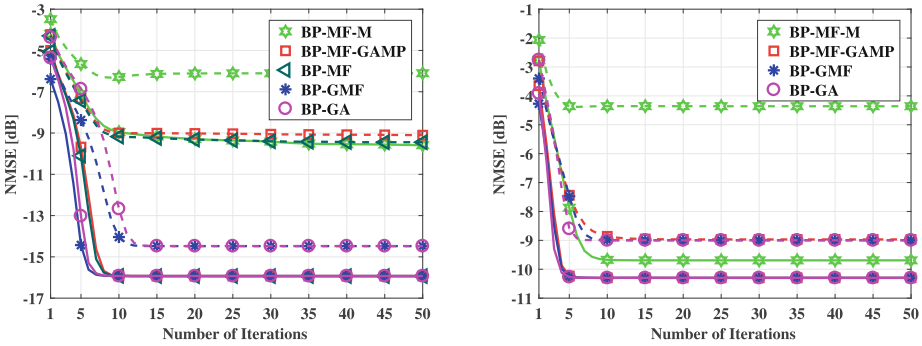

(a) 16×8 (b) 64×8

Fig. 4. NMSE of time-domain channel taps versus number of turbo iterations, under $E_\mathrm{b}/N_0 = 7.25\,\mathrm{dB}$ (dashed lines) and $E_\mathrm{b}/N_0 = 8.75\,\mathrm{dB}$ (solid lines).

$$\mathsf{NMSE} = \frac{1}{\Theta}\sum_{\theta=1}^{\Theta}\frac{1}{MN}\sum_{m=1}^{M}\sum_{n=1}^{N}\frac{\sum_{l=1}^{L}\left|h_{mnl}-\hat{h}_{mnl}^{(i)}\right|^2}{\sum_{l=1}^{L}\left|h_{mnl}\right|^2}, \tag{37}$$

where Θ is the number of Monte Carlo runs.

Figure 3 shows the normalized mean-squared error of the channel estimation versus E_b/N_0 in the 16×8 MIMO system and the 64×8 MIMO system, respectively. It is shown that the NMSE of the proposed BP-GMF outperforms the MMSE, the BP-MF-M, the BP-MF-GAMP and the BP-MF (which is evaluated only in the 16×8 MIMO system due to complexity issue) in both cases.

Figure 4 presents the NMSE performance versus the number of turbo iterations. Results indicate that the BP-GMF and BP-GA demonstrate almost the same convergency, and need less than 15 iterations to converge.

4.2 BER Versus E_b/N_0

Figure 5 shows the BER performance versus E_b/N_0 in the 16×8 MIMO system and the 64×8 system, respectively. The BP-GA algorithm and BP-GMF algorithm achieve the same performance that is about 0.8 dB away from the MFB-PCSI at BER $= 10^{-5}$; the BP-MF algorithm slightly outperforms the BP-MF-GMP algorithm, but its performance is about 1.3 dB away from the MFB-PCSI at BER $= 10^{-5}$.

Figure 6 presents the BER performance versus the number of turbo iterations. Results indicate that the BP-GMF and BP-GA demonstrate almost the same convergency, and need less than 15 iterations to converge.

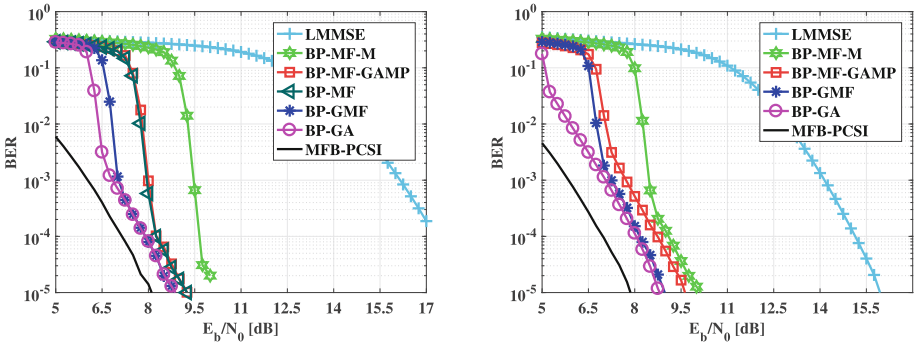

(a) 16×8 (b) 64×8

Fig. 5. BER versus E_b/N_0 in MIMO systems with 16QAM.

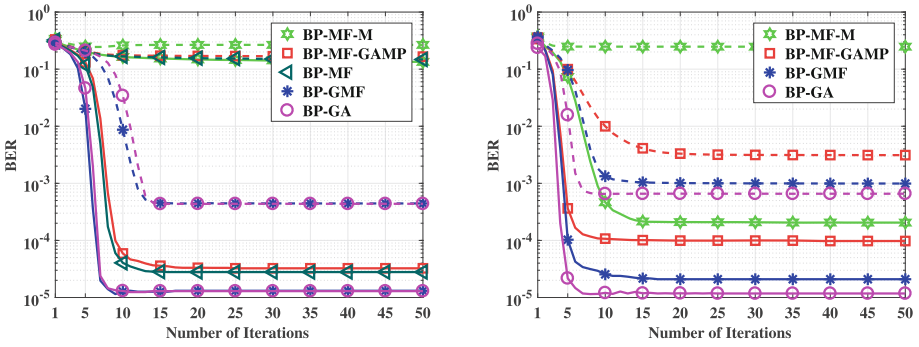

(a) 16×8 (b) 64×8

Fig. 6. BER versus number of turbo iterations, under $E_b/N_0 = 7.25$ dB (dashed lines) and $E_b/N_0 = 8.75$ dB (solid lines).

5 Conclusion

In this paper, a message-passing scheme combining LBP with Gaussian approximation and mean-field approximation is proposed for massive MIMO-OFDM systems. Simulation results show that the proposed scheme can achieve the performance of the BP-GA, within 0.8 dB of the known-channel bound in a 16×8 MIMO system and a 64×8 MIMO system, and outperforms the BP-MF and its low-complexity variants considerably.

References

1. Marzetta, T.L.: Noncooperative cellular wireless with unlimited numbers of base station antennas. IEEE Trans. Wirel. Commun. **9**(11), 3590–3600 (2010)
2. Wang, S., Li, Y., Zhao, M., Wang, J.: Energy efficient and low-complexity uplink transceiver for massive spatial modulation MIMO. IEEE Trans. Veh. Technol. **PP**(99), 1–1 (2014)
3. Wu, S., Kuang, L., Ni, Z., Lu, J., (David) Huang, D., Guo, Q.: Expectation propagation based iterative groupwise detection for large-scale multiuser MIMO-OFDM systems. In: Proceedings of IEEE Wireless Communications and Networking Conference (WCNC), pages 248–253, April 2014
4. Wang, S., Li, Y., Wang, J.: Multiuser detection in massive spatial modulation MIMO with low-resolution ADCs. IEEE Trans. Wirel. Commun. **14**(4), 2156–2168 (2015)
5. Liu, L., Yuen, C., Guan, Y.L., Li, Y., Su, Y.: A low-complexity Gaussian message passing iterative detector for massive MU-MIMO systems. In: 2015 10th International Conference on Information, Communications and Signal Processing (ICICS), pp. 1–5, December 2015
6. Liu, L., Yuen, C., Guan, Y.L., Li, Y., Su, Y.: Convergence analysis and assurance for Gaussian message passing iterative detector in massive MU-MIMO systems. IEEE Trans. Wirel. Commun. **15**(9), 6487–6501 (2016)
7. Dai, L., Wang, Z., Yang, Z.: Spectrally efficient time-frequency training OFDM for mobile large-scale MIMO systems. IEEE J. Sel. Areas Commun. **3**(2), 251–263 (2013)
8. Rossi, P.S., Müller, R.R.: Joint twofold-iterative channel estimation and multiuser detection for MIMO-OFDM systems. IEEE Trans. Wirel. Commun. **7**(11), 4719–4729 (2008)
9. Novak, C., Matz, G., Hlawatsch, F.: IDMA for the multiuser MIMO-OFDM uplink: a factor graph framework for joint data detection and channel estimation. IEEE Trans. Sig. Process. **61**(16), 4051–4066 (2013)
10. Wu, S., Ni, Z., Meng, X., Kuang, L.: Block expectation propagation for downlink channel estimation in massive MIMO systems. IEEE Commun. Lett. **20**(11), 2225–2228 (2016)
11. Lin, X., Wu, S., Kuang, L., Ni, Z., Meng, X., Jiang, C.: Estimation of sparse massive MIMO-OFDM channels with approximately common support. IEEE Commun. Lett. **PP**(99), 1 (2017)
12. Kschischang, F.R., Frey, B.J., Loeliger, H.-A.: Factor graphs and the sum-product algorithm. IEEE Trans. Inf. Theor. **47**(2), 498–519 (2001)
13. Worthen, A.P., Stark, W.E.: Unified design of iterative receivers using factor graphs. IEEE Trans. Inf. Theor. **47**(2), 843–849 (2001)

14. Liu, Y., Brunel, L., Boutros, J.J.: Joint channel estimation and decoding using Gaussian approximation in a factor graph over multipath channel. In: Proceedings of the International Symposium on Personal, Indoor and Mobile Radio Communication (PIMRC), pp. 3164–3168 (2009)
15. Kirkelund, G.E., Manchón, C.N., Christensen, L.P.B., Riegler, E., Fleury, B.H.: Variational message-passing for joint channel estimation and decoding in MIMO-OFDM. In: Proceedings of IEEE Global Telecommunications Conference (GLOBECOM), pp. 1–6 (2010)
16. Guo, Q., (David) Huang, D.: EM-based joint channel estimation and detection for frequency selective channels using Gaussian message passing. IEEE Trans. Sig. Process. **59**(8), 4030–4035 (2011)
17. Schniter, P.: A message-passing receiver for BICM-OFDM over unknown clustered-sparse channels. IEEE J. Sel. Top. Sig. Process. **5**(8), 1462–1474 (2011)
18. Knievel, C., Hoeher, P.A., Tyrrell, A., Auer, G.: Multi-dimensional graph-based soft iterative receiver for MIMO-OFDM. IEEE Trans. Commun. **60**(6), 1599–1609 (2012)
19. Riegler, E., Kirkelund, G.E., Manchón, C.N., Badiu, M.-A., Fleury, B.H.: Merging belief propagation and the mean field approximation: a free energy approach. IEEE Trans. Inf. Theor. **59**(1), 588–602 (2013)
20. Wu, S., Kuang, L., Ni, Z., Lu, J., (David) Huang, D., Guo, Q.: Expectation propagation approach to joint channel estimation and decoding for OFDM systems. In: Proceedings of IEEE International Conference on Acoustics, Speech, and Signal Processing (ICASSP), pp. 1941–1945, May 2014
21. Schniter, P.: Joint estimation and decoding for sparse channels via relaxed belief propagation. In: Proceedings of the 44th Asilomar Conference on Signals, Systems and Computers (ASILOMAR), pp. 1055–1059. IEEE (2010)
22. Manchón, C.N., Kirkelund, G.E., Riegler, E., Christensen, L.P.B., Fleury, B.H.: Receiver architectures for MIMO-OFDM based on a combined VMP-SP algorithm. arXiv:1111.5848 (2011)
23. Badiu, M.-A., Kirkelund, G.E., Manchón, C.N., Riegler, E., Fleury, B.H.: Message-passing algorithms for channel estimation and decoding using approximate inference. In: Proceedings of IEEE International Symposium on Information Theory (ISIT), pp. 2376–2380 (2012)
24. Drémeau, A., Herzet, C., Daudet, L.: Boltzmann machine and mean-field approximation for structured sparse decompositions. IEEE Trans. Sig. Process. **60**(7), 3425–3438 (2012)
25. Krzakala, F., Manoel, A., Tramel, E.W., Zdeborová, L.: Variational free energies for compressed sensing. In: Proceedings of IEEE International Symposium on Information Theory (ISIT), pp. 1499–1503, June 2014
26. Badiu, M.-A., Manchón, C.N., Fleury, B.H.: Message-passing receiver architecture with reduced-complexity channel estimation. IEEE Commun. Lett. **17**(7), 1404–1407 (2013)
27. Yuan, Z., Zhang, C., Wang, Z., Guo, Q., Wu, S., Wang, X.: A low-complexity receiver using combined BP-MF for joint channel estimation and decoding in OFDM systems. CoRR, abs/1601.05856 (2016)
28. Wu, S., Kuang, L., Ni, Z., Lu, J., (David) Huang, D., Guo, Q.: Low-complexity iterative detection for large-scale multiuser MIMO-OFDM systems using approximate message passing. IEEE J. Sel. Top. Sig. Process. **8**(5), 902–915 (2014)
29. Meng, X., Wu, S., Kuang, L., Ni, Z., Lu, J.: Expectation propagation based iterative multi-user detection for MIMO-IDMA systems. In: 2014 IEEE 79th Vehicular Technology Conference (VTC Spring), pp. 1–5, May 2014

30. Meng, X., Wu, S., Kuang, L., Lu, J.: An expectation propagation perspective on approximate message passing. IEEE Sig. Process. Lett. **22**(8), 1194–1197 (2015)
31. Minka, T.P.: Divergence measures and message passing. Technical report MSR-TR-2005-173, Microsoft Research Ltd., Cambridge, UK, December 2005
32. Wu, S., Kuang, L., Ni, Z., Huang, D., Guo, Q., Lu, J.: Message-passing receiver for joint channel estimation and decoding in 3D massive MIMO-OFDM systems. IEEE Trans. Wirel. Commun. **15**(12), 8122–8138 (2016)
33. Hochwald, B.M., ten Brink, S.: Achieving near-capacity on a multiple-antenna channel. IEEE Trans. Commun. **51**(3), 389–399 (2003)